Split-disk micro-lasers: Tunable whispering gallery mode cavities

T. Siegle, M. Remmel, S. Krämmer, and H. Kalt

Articles you may be interested in

An actively controlled silicon ring resonator with a fully tunable Fano resonance
APL Photonics **2**, 096101 (2017); 10.1063/1.5000514

Ultra-high Q/V hybrid cavity for strong light-matter interaction
APL Photonics **2**, 086101 (2017); 10.1063/1.4994056

Exact solution to the steady-state dynamics of a periodically modulated resonator
APL Photonics **2**, 076101 (2017); 10.1063/1.4985381

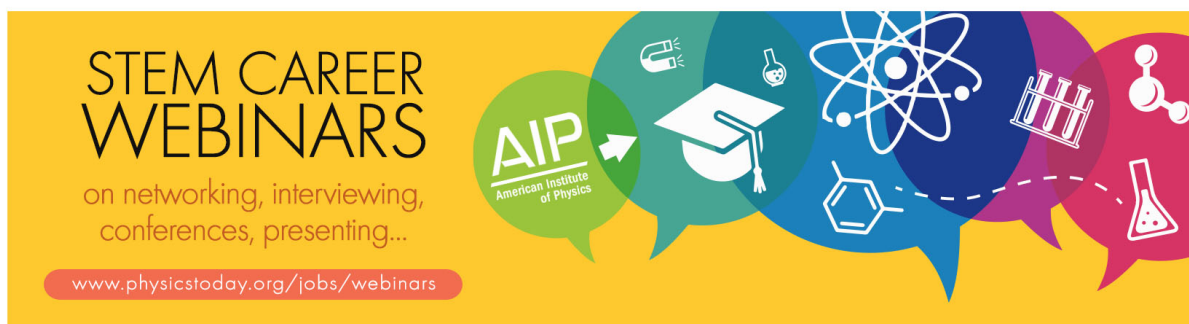Integrating cell on chip—Novel waveguide platform employing ultra-long optical paths
APL Photonics **2**, 096102 (2017); 10.1063/1.5001486

Ultra-compact visible chiral spectrometer with meta-lenses
APL Photonics **2**, 036103 (2017); 10.1063/1.4974259

Recommendations and illustrations for the evaluation of photonic random number generators
APL Photonics **2**, 090901 (2017); 10.1063/1.5000056

Split-disk micro-lasers: Tunable whispering gallery mode cavities

T. Siegle,[a] M. Remmel, S. Krämmer, and H. Kalt
Institute of Applied Physics, Karlsruhe Institute of Technology, 76128 Karlsruhe, Germany

Optical micro-cavities of various types have emerged as promising photonic structures, for both the investigation of fundamental science in cavity quantum electrodynamics and simultaneously for various applications, e.g., lasers, filters, or modulators. In either branch a demand for adjustable and tunable photonic devices becomes apparent, which has been mainly based on the modification of the refractive index of the micro-resonators so far. In this paper, we report on a novel type of whispering gallery mode resonator where resonance tuning is achieved by modification of the configuration. This is realized by polymeric split-disks consisting of opposing half-disks with an intermediate air gap. Functionality of the split-disk concept and its figures of merit like low-threshold lasing are demonstrated for laser dye-doped split-disks fabricated by electron beam lithography on Si substrates. Reversible resonance tuning is achieved for split-disks structured onto elastomeric substrates by direct laser writing. The gap width and hence the resonance wavelength can be well-controlled by mechanically stretching the elastomer and exploiting the lateral shrinkage of the substrate. We demonstrate a broad spectral tunability of laser modes by more than three times the free spectral range. These cavities have the potential to form a key element of flexible and tunable photonic circuits based on polymers. *© 2017 Author(s). All article content, except where otherwise noted, is licensed under a Creative Commons Attribution (CC BY) license (http://creativecommons.org/licenses/by/4.0/).* [http://dx.doi.org/10.1063/1.4985766]

I. INTRODUCTION

Optical micro-cavities have enormously promoted research progress in optics in recent years. They have arisen as promising photonic structures in both fundamental science, e.g., in the field of cavity quantum electrodynamics[1–3] or cavity opto-mechanics[4,5] and simultaneously in a variety of different applications, e.g., as optical sensors,[6–10] as low-threshold lasers,[11–13] or as filters or modulators in optical telecommunication.[14–16]

Several different embodiments of micro-cavities have emerged ranging from Fabry-Pérot cavities, photonic crystals and distributed feedback (DFB) cavities to whispering gallery mode (WGM) resonators.[1,17] For all types of micro-cavities, the resonance frequency is dictated by the resonator design and the refractive index of the cavity. Without the possibility to modify these parameters, the resonances of a micro-cavity are inherently fixed and the devices are inflexible regarding optical tuning.

However, flexible and tunable devices are highly desirable. They are required to intentionally match the resonance with an optical transition of an interacting quantum emitter,[18,19] a prerequisite for the observation of strong light-matter coupling.[20] In the case of coupling resonators to photonic molecules, mode matching is essential for a coherent photon transfer between the cavities.[21] Likewise, the functionality of applications as filters, modulators, switches, or routers are strongly enhanced— given the possibility to adjust the resonator properties.

---

[a]Author to whom correspondence should be addressed: tobias.siegle@kit.edu

As previously mentioned, there are basically two ways of influencing the resonances, either by modulation of the cavity material or by variation of the size of the cavity. Most tunable micro-cavities rely on a variation of the refractive index of the cavity material, either by electro-optical or thermo-optical modulation. For polymers, e.g., PMMA with relatively large thermo-optic coefficient,[22] thermo-optical variation of the refractive index is typically applied with a possible detuning of the resonance wavelength of some tens of picometer per Kelvin. For electro-optic polymers, a detuning of some picometer per volt can be achieved.[16] For semiconductor devices, additionally an injection of free-carriers can be applied to alter the refractive index.[15,23,24] While tuning based on the electro-optical effect and free-carrier dispersion effect can be realized at high speed, the tuning range is rather small. Conversely, thermal tuning operates with low or moderate speed, but typically possesses larger tuning ranges.[25]

Whereas a variation of the refractive index can be applied to all types of cavities, the second possibility, i.e., addressing the geometry of the cavity and tuning the resonances by modifying the structure, is prohibited in most types of cavities due to the employed materials. For monolithic devices made from, e.g., glasses or semiconductors, a nondestructive deformation of the cavity shape is not feasible as the structures are inherently inflexible — linked to the rigidity of both the material of the cavity and the used substrates.

One interesting approach is based on the incorporation of MEMS (micro-electrical mechanical systems) into photonic devices to yield resonance tuning. In this way tunable optical filters have been realized based on a MEMS-controlled change of the length of a Fabry-Pérot cavity;[26] similarly, tunable lasers made from micromechanically tunable VCSEL (vertical cavity surface emitting laser) have been presented.[27] MEMS actuators are also in use to adjust the coupling ratio between micro-cavities and external waveguides.[28] Dynamic add-drop filters[29] and slow-light in optical delay lines[30] could be realized in that way.

Tuning of individual WGM resonators can be achieved by a size reduction of WGM cavities by photo-electrochemical etching, where the dielectric medium that forms the cavity is partly etched in the presence of light resonating in the cavity.[31] Tuning without material removal and reversible shape variation is not straightforward and has not been realized so far except for very few approaches based on polymer devices, e.g., for polymer droplets integrated into polydimethylsiloxane (PDMS)[32] or liquid crystal elastomers embedded into PMMA micro-goblets[33] (see below). By structuring Bragg gratings onto elastomeric substrates (e.g., PDMS), tunable DFB devices can be realized. A deformation of the substrate results in a variation of the grating pitch and thus the resonance wavelength. Typically, a mechanical substrate deformation[34–36] is applied; however, for electroactive materials also an electrical tuning has been achieved.[37] Tunable elastomer DFB lasers are realized not only in combination with liquid active materials, e.g., with the aid of dye solutions,[34] but also in solid-state polymeric devices with embedded emitters.[35,37]

In this context, the trendsetting concept of using polymers and elastomers for photonic devices becomes apparent as they provide an alternative approach to tunability. In this novel branch of "tunable polymer photonics," we have already performed some key experiments revealing the potential of tunability in WGM micro-resonators: Recently, we have presented a way to modify the resonator shape of a polymeric micro-cavity and hence to control the resonances of a micro-goblet optically by exploiting the anisotropic expansion of liquid crystal elastomers. Tuning of individual micro-resonators over more than one free spectral range is feasible, however, needs complex, time-consuming and individual integration of polymerized liquid crystal elastomer cylinders into each single micro-goblet.[33] In the context of flexible coupling between micro-cavities in photonic molecules, the crucial point is to influence the inter-cavity coupling gap. Up to the coupling of two resonators, this is feasible by using nano-positioning systems.[21,38] For such tuning in larger cavity arrays, we have established an alternative platform by structuring the cavity arrays onto elastomeric substrates.[39]

Elaborating this approach, we present here a novel type of a WGM micro-resonator with a wide tuning range and with the prospect of easy integration into cavity arrays: Polymeric split-disk resonators. They consist of opposing half-disks with an intermediate air gap, structured with either electron beam lithography or 3D lithography (direct laser writing, DLW). Resonance tuning is achieved by reversible mechanical deformation of the elastomer substrate enabling precise control of

the air gap.[40] In the following, we first focus on the demonstration of the functionality of split-disk micro-resonators and then prove resonance tuning over a broad spectral range.

II. FABRICATION, OPERATION, AND CHARACTERIZATION METHODS

A. Lithographic fabrication of polymeric split-disk resonators

Initial tests of the basic functionality of split-disks as WGM resonators have been performed on opposing half-disks structured following a well-engineered fabrication process.[41] The resonators were patterned into a positive-tone resist based on poly(methyl methacrylate) (PMMA 950K A6, Micro Resist Technology GmbH, Berlin, Germany) by electron beam lithography on rigid silicon substrates. After chemical development the silicon was isotropically etched using xenon difluoride.

To investigate resonance tuning we structured split-disks by 3D lithography into a homemade negative-tone resist based on the monomer pentaerythritol triacrylat (PETA, Sigma-Aldrich Chemie GmbH, Munich, Germany) mixed with 2 wt. % of Irgacure® 819 (BASF SE, Germany) as photo-initiator. Rather than rigid silicon substrates, we now use elastomeric polydimethylsiloxane (PDMS, SYLGARD 184 Silicone Elastomer, Dow Corning GmbH, Wiesbaden, Germany). The preparation of PDMS substrates, the necessary pre-treatment to enhance its adhesion properties, the DLW structuring, and development process are identical to the process described by Siegle *et al.* in an earlier publication.[39]

Polymers can be easily doped with organic dyes to from active resonators, e.g., ring resonator lasers[42] or disk and goblet lasers.[12] Following these approaches to form active micro-resonators that enable lasing emission through optical pumping (see below), both types of photo-resists were doped with the laser dye Pyrromethene 597 (Radiant Dyes Laser & Accessories GmbH, Wermelskirchen, Germany) at a concentration of 25 μmol prior to the structuring process.

Non-flexible split-disks on silicon pedestals are fabricated with designed coupling gaps d between 200 nm and 1800 nm in steps of 200 nm resulting in gap separations between 660 nm and 2200 nm after completing the fabrication process (determined by SEM images). Split-disks on PDMS are structured with an initial coupling gap of several microns. Illustrating SEM images are depicted in Fig. 1(a) for a split-disk made by electron beam lithography and in Fig. 1(b) for the fabrication with DLW. Concerning the experimentally achievable coupling gap, electron beam lithography is clearly superior to DLW, however, impedes patterning on non-conductive substrates. Here, DLW is advantageous as it can be applied independently of the substrate, i.e., also on elastomers for enabling tuning of the gap as presented in the following.

B. Tuning of the gap between opposing half-disks

Derived from the resonance condition of rotationally symmetric WGM micro-cavities,[43] for a split-disk geometry, the following modified formula applies, including the intermediate coupling gap d between opposing half-disks,

$$2\pi R \times n_\mathrm{c} + 2d \times n_\mathrm{gap} \approx m\lambda, \tag{1}$$

with n_c and n_gap describing the refractive indices of the cavity material and the gap, respectively. The azimuthal quantum number is denoted by m while λ is the resonance wavelength. Equation (1) represents an approximation for the resonance condition as in a strict sense the effective refractive index of the WGM has to be applied. However, due to the relatively large index contrast between polymer and air, one can use the cavity refractive index and the geometrical light path as a good approximation. This allows us to compare experimentally determined cavity characteristics, e.g., free spectral range, with theoretical expectations without performing elaborate simulations. Influencing the cavity by varying d inevitably modifies the resonance wavelength λ as can be seen from Eq. (1).

For this purpose we use an approach based on mechanical deformation of the elastomer substrate that has been used earlier for the realization of photonic molecules with tunable inter-cavity coupling gaps.[39] Therefore, the PDMS substrate is fixed between clamps and mechanically elongated using a micrometer screw. If the gap of a split-disk is structured orienting along the stretching direction, the gap distance can be reduced by exploiting the lateral contraction as illustrated in Fig. 1(c).
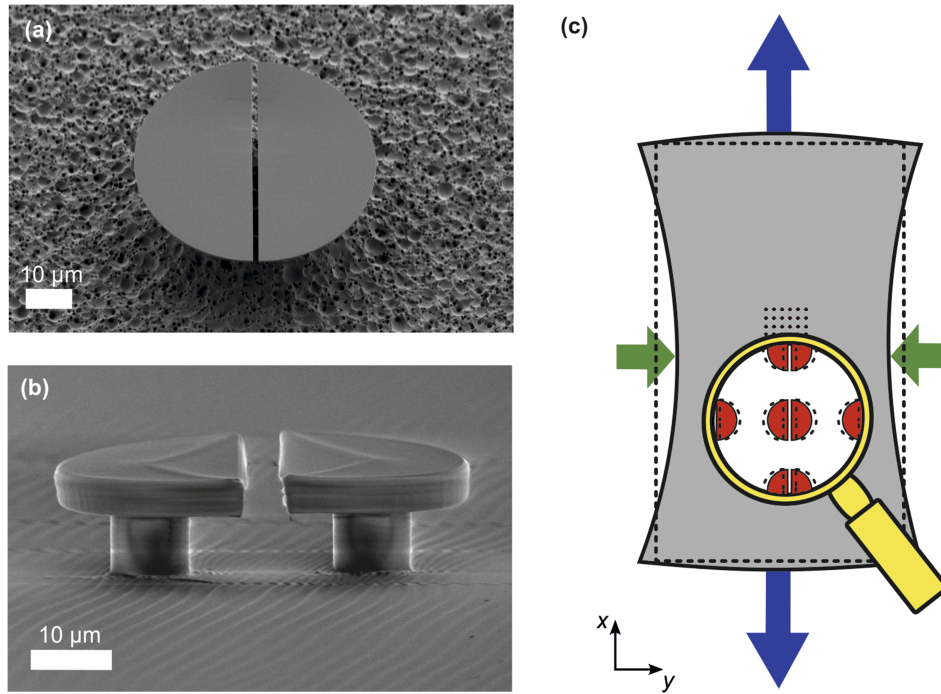
FIG. 1. (a) Scanning electron micrograph of a PMMA split-disk consisting of opposing half-disks of radius $r = 25\ \mu$m and an intermediate coupling gap of $d = 1200$ nm patterned by electron-beam lithography on a silicon substrate. (b) Scanning electron image of a polymeric split-disk ($r = 25\ \mu$m, $d = 4.5\ \mu$m) fabricated by direct laser writing on a PDMS elastomer substrate. (c) Illustration of the coupling process: Mechanically stretching the substrate in x-direction (blue arrows) results in a lateral contraction in y-direction (green arrows) and consequently in a reduction of the gap width between the opposing half-disks. The dotted lines illustrate the pre-stretching state, whereas the red, filled half-disks represent the opposing half-disks with a reduced gap after applying substrate strain. (b) and (c) based on Ref. 40.

Important is now to calibrate the actual gap size since it cannot be determined directly during the optical experiments. The calibration method used in Ref. 39, where the distortions of an imprinted square mesh are evaluated, shows that the lateral contraction is linearly dependent on the substrate elongation since the deformations occur in the elastic regime. Having confirmed this we can actually use our optical experiments for calibration of the gap size. Later (in Fig. 5) we prove by fitting straight lines to the experimental data that the modal shifts $\Delta\lambda$ also depend linearly on the substrate elongation Δx. Since the resonance wavelength on the other hand is linearly dependent on the gap size d [see Eq. (1)], we can relate the measured modal shift $\Delta\lambda$ to the elongation Δx and thus to change of gap size Δd by

$$\Delta d = \Delta\lambda \times \frac{d}{\lambda} \times \frac{\pi R n_{\mathrm{c}} + d n_{\mathrm{gap}}}{d n_{\mathrm{gap}}}, \tag{2}$$

and using $\Delta\lambda = \pm 5.5$ pm/μm $\times \Delta x$ deduced from the linear dependencies shown in Fig. 5, for stretching and relaxation of the substrate, respectively. Equation (2) is derived from Eq. (1) by differentiating λ with respect to d. For the linear dependence between the change of the gap width Δd and the substrate elongation Δx, we find $\Delta d = \pm 1.15$ nm/μm $\times \Delta x$. See supplementary material for more details. This optical calibration method is a highly useful byproduct of our studies demonstrating that split-disk resonators can be employed for calibrations of flexible photonic architectures.

C. Optical characterization with photoluminescence spectroscopy

Dye-doped micro-resonators can be characterized in a free-space optical setup by micro-photoluminescence spectroscopy. A frequency-doubled Nd:YVO$_4$ laser emitting 10-ns pulses at a repetition rate of 20 Hz and a wavelength of 532 nm is used as a pump laser and focused on the micro-cavities at an angle of roughly 45°. Photoluminescence is collected perpendicular to the micro-cavities with a microscope objective (NA = 0.4, 50×) and analyzed in a spectrometer equipped

with a CCD camera. A more detailed description of the setup and a schematic can be found in the supplementary material.

D. Determination of the Q-factor in transmission measurements

The Q-factor of a split-disk resonator is determined from transmission spectra of light guided through a tapered optical fiber that has been closely approached to the resonator rim. The quality factor is given by the linewidth of the resonance dips resulting from coupling the light into the cavity. A corresponding schematic of the setup and a more detailed description can be found in the supplementary material.

III. RESULTS AND DISCUSSION

To demonstrate the basic functionality of split-disks and the feasibility of their application as tunable WGM micro-resonators, the two different realizations of WGM split-disks are optically characterized in the following. First, we report on the influence of splitting disks into two parts on the lasing threshold and quality factor for the devices with fixed gap; afterwards, we focus on resonance tuning of split-disks patterned on elastomeric PDMS substrates.

A. Split-disk micro-cavities–An alternative WGM geometry

Laser emission from fixed-gap split-disks made by electron beam lithography is used to characterize the resonator properties. Lasing is verified from the distinct kink in the input-output characteristics curve accompanied by the occurrence of spectrally sharp emission peaks on top of the spontaneous dye fluorescence as illustrated in Fig. 2(a). From the pump energy dependence of the lasing mode evolving at the lowest pump energy density (highlighted in red in the inset), we can infer the lasing threshold of the split-disk ($E_{th, d=1200\,nm} = 480\ \mu J\ pulse^{-1}\ cm^{-2}$) for the shown split-disk with a gap of $d = 1200$ nm.

The lasing spectrum in the inset of Fig. 2(a) and comparable spectra for split-disks with other gap widths [see Fig. 3(b)] reflect that mainly fundamental modes buildup. Higher-order modes, which are frequently observed in non-split PMMA micro-disks, occur only rarely since they are suppressed by the additionally introduced losses at the gap.[44] The free spectral range can be determined to be $FSR_{exp} = 1.43$ nm, which corresponds well with the theoretically expected $FSR_{theo} = 1.45$ nm at 585 nm. No lasing emission could be detected from individually structured, single dye-doped half-disks, but only from opposing half-disks. The coinciding free spectral ranges and the lasing inability
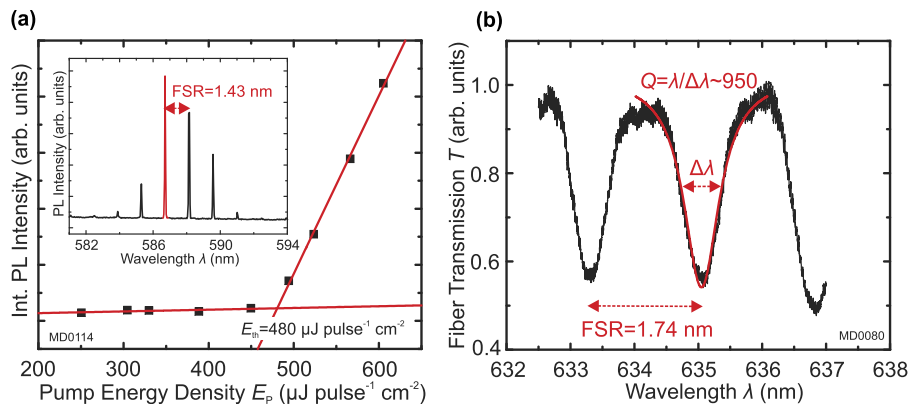

FIG. 2. (a) Input-output curve of a dye-doped PMMA split-disk micro-laser with a fixed gap of $d = 1200$ nm fabricated by electron beam lithography. The lasing threshold of $E_{th} = 480\ \mu J\ pulse^{-1}\ cm^{-2}$ is determined from the kink in the integrated PL intensity of the mode evolving at the lowest energy. The inset shows a corresponding PL spectrum above the lasing threshold with fundamental modes separated by the free spectral range of FSR = 1.43 nm around 585 nm. The mode evaluated for the determination of the threshold is marked in red. (b) Transmission spectrum through a tapered optical fiber aligned to a WGM split-disk ($d = 1200$ nm). A Lorentzian has been fitted to determine the resonator quality factor of $Q \sim 950$ and the free spectral range of FSR = 1.74 nm around 635 nm.
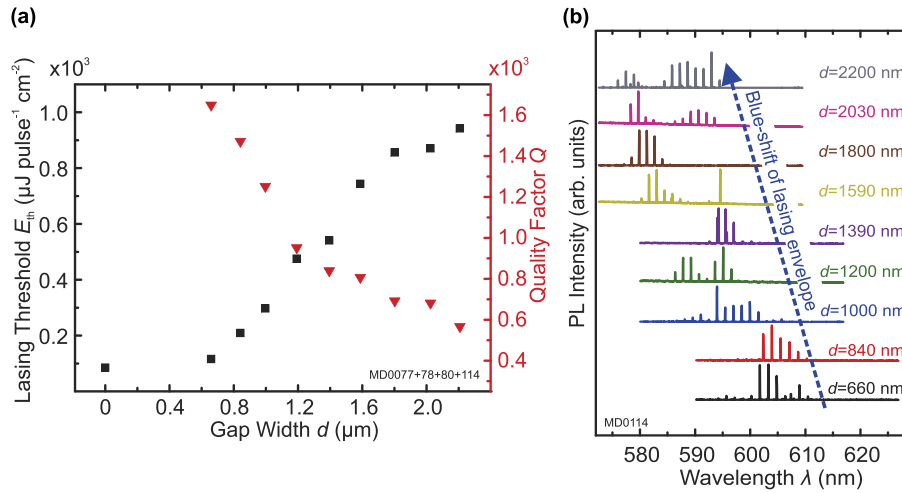
(a)

(b)

FIG. 3. (a) Dependence of the lasing threshold (black squares) and the quality factor (red triangles) on the gap separation d. An increase of the lasing threshold is identified that is linked to increased cavity losses as confirmed from an opposing trend of the quality factor recorded in transmission measurements. For purposes of presentation we left out the quality factor for non-split-disks ($Q_{d=0\,nm} = 2.1 \times 10^4$). (b) By stacking PL spectra for various gap widths d, a blue-shift of the lasing mode envelope can be recognized that is also related to the decrease of the quality factor.

of individual half-disks confirm the lasing emission to originate from whispering gallery modes and prove the basic functionality of split-disks as whispering gallery mode resonators.

An important cavity figure of merit is the Q-factor. The latter is determined from transmission of light through a tapered fiber coupled to the cavity. The light wavelength is chosen to be well below the onset of the absorption by the incorporated laser dye. We show a typical example in Fig. 2(b) for a split-disk with a gap of $d = 1200$ nm. The deduced free spectral range $FSR_{exp} = 1.74$ nm corresponds again well to its expected value $FSR_{theo} = 1.72$ nm at a wavelength of 635 nm. The quality factor has been determined to be $Q \sim 950$. This value is about a factor of 20 lower than the one for comparable dye-doped disks without split gap ($Q_{d=0\,nm} = 2.1 \times 10^4$) but still high enough for a good laser cavity.

We now want to characterize how the gap size between the half-disks affects the lasing threshold and the quality factor. For this we studied the lasing from split-disks with different (fixed) gap widths. The resulting thresholds (averaged over several resonators) are presented in Fig. 3(a). Clearly an increase of the lasing threshold with increasing gap width can be identified. This increase has two origins: First, by increasing the path through the non-doped gap which does not experience any optical gain, the overall gain in the cavity system is reduced and hence the lasing threshold should be increased. Another reason for the increasing threshold is attributed to rising losses within the air gap where the mode is not confined (see below). Remarkably, the lasing threshold of split-disks with a gap of $d = 2200$ nm ($E_{th,d=2200\,nm} = 940\ \mu J\ pulse^{-1}\ cm^{-2}$) has only increased by a factor of eleven compared to micro-disks without any gap ($E_{th,d=0\,nm} = 85\ \mu J\ pulse^{-1}\ cm^{-2}$). This shows that active split-disks retain their character of low-threshold lasers even for large gap sizes.

To verify that the increase of lasing threshold is indeed linked to an increase of losses, we performed transmission measurements for the various split-disks of different gap widths as explained above. Together with the lasing threshold, the measured quality factors are presented in Fig. 3(a) (red triangles). Opposing trends of quality factor and lasing threshold are observed reflecting the interrelated behavior of these quantities.[45]

Also consistent with the latter findings is the observation that the gap size influences the spectral position of the WGM lasing. As illustrated in Fig. 3(b), a blue-shift of the spectral envelope of the lasing peaks by more than 10 nm is observed. This behavior can again be linked to the change in cavity Q-factor and is a well-understood phenomenon. Such blue shifts are well documented in dye-based micro-lasers for increasing absorption[45] or radiation losses.[32,46,47] In the presented work losses affecting the quality factor are due to the decreasing confinement in the gap region [see Fig. 3(a)].

To sum up this first part, we have shown that although splitting dye-doped micro-disks negatively affects the quality of the cavity, the figures of merit are still sufficient and the functionality as low-threshold WGM laser is maintained. This is a crucial point for the realization of tunability in such micro-lasers, as shown in the following.

B. Realization of tunable micro-lasers on elastomer substrates

In this section we demonstrate the capability of a broad spectral tunability of cavity resonances when split-disk resonators are patterned by DLW onto an elastomer substrate. The flexibility of the substrate enables a smooth and well-controllable variation of the resonator gap and thus of the resonance wavelength [Eq. (1)]. For this purpose, a PDMS substrate was mechanically stretched in order to exploit the lateral substrate contraction as described above [see Fig. 1(b)].

We show exemplary results for a split-disk with a radius of $r = 25.4$ μm and an initial gap size of $d_{\text{initial}} = 2580$ nm as determined from SEM images. Just as in the case of fixed-gap cavities on silicon, if excited above lasing threshold, fundamental lasing modes separated by the FSR can be identified [see Fig. 4(a)]. For the shown spectra we find experimentally a free spectral range of $\text{FSR}_{\text{exp}} = 1.35$ nm. As can be seen in the zoom-in in Fig. 4(b), two mode families are present. The second mode comb is also present in Fig. 4(a), however, cannot be recognized in the normalized spectrum due to large differences of the lasing intensities. The lasing thresholds of split-disks made by DLW are actually increased by roughly one order of magnitude compared to the cavities fabricated by electron beam lithography. This factor was also found for regular, non-split polymeric micro-disks and is mainly attributed to the effect of photo-bleaching and aggregation of dye molecules originating from the high incident power in the two photon absorption process.[12,48–50]

Let us first focus on implementation, precision, and reproducibility of our tuning experiments. Starting at the initial value $d_{\text{initial}} = 2580$ nm, the gap has been gradually reduced by applying increasing substrate elongation in steps of $\Delta x = 50$ μm up to a maximum of $\Delta x_{\text{max}} = 800$ μm. Following our calibration method[39] and Eq. (2) given above, this translates in the perpendicular direction into changes of the gap size of $\Delta d = -57.5$ nm and a maximum change of $\Delta d_{\text{max}} = -920$ nm. In principle even a much larger tuning is possible as the initial gap width is $d_{\text{initial}} = 2580$ nm and since also larger substrate elongations keep up the linear elastic regime.[39] But here, the substrate was not stretched to the extreme as the gap widths cannot be imaged directly during the measurement and we wanted to avoid touching of the resonator halves. Exemplary, lasing spectra recorded from the split-disk resonator for $\Delta d = -57.5$ nm (blue line), -115 nm (red line), and -172.5 nm (black line)
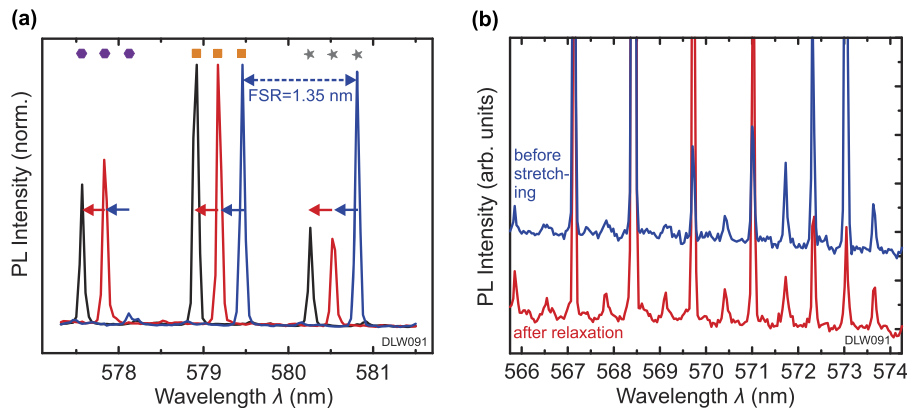

FIG. 4. (a) PL spectra of dye-doped polymeric split-disks made by DLW. Lasing modes separated by the free spectral range are visible. Applying increasing substrate strain results in a reduction of the gap size $\Delta d = -57.5$ nm (blue line), -115 nm (red line), and -172.5 nm (black line) that evokes a blue-shift of the lasing modes (indicated with blue and red arrows). To link the presented lasing modes to Fig. 5, we mark them by corresponding symbols (purple hexagon, orange square, and grey star). (b) PL spectra before applying strain (blue line) and after relaxation of the substrate (red line): Although the lasing intensity fluctuates, it can be seen that the lasing modes are located at the same spectral position demonstrating the full reversibility of our tuning approach.

are displayed in Fig. 4(a). The blue-shift expected from the reduction of the gap size according to Eq. (1) is obvious. The above mentioned second mode family experiences identical blue-shifts.

Here we need to comment on the fluctuations of the laser-mode intensity or even an occasional disappearance of a mode upon changing the gap. This does not result from spectral modifications or variations of the modal losses. The observations are due to the particular method of recording the lasing spectra. This is done in free-space optics collecting the light scattered from the disks perpendicular to the plane of disk and then cutting out only a small area of the resonator by imaging the disks onto the entrance slit of the spectrometer.[44,48] Such collection is straightforward and simple to implement but relies on imperfections of the disk surface that scatter the light towards the collecting optics. Due to the deformation of the substrate, the position of the resonator and thus the imperfections with respect to the spectrometer entrance slit slightly vary causing the observed intensity fluctuations. Such intensity fluctuations can strongly be reduced by collecting light emitted from the resonator rim in the disk plane (radiative loss of the cavity) or when collecting (and exciting) the laser light by fiber coupling. Anyways, the focus of this report is the large tunability of the resonances which is demonstrated unambiguously.

In order to elaborate the dependence of the modal shift on the gap size, we have determined the spectral positions of the lasing modes by fitting Lorentzian functions to the corresponding peaks. The precision of the spectral fine-tuning of the resonances is evaluated to be approximately $\Delta\lambda \sim 25$ pm assuming minimum steps of substrate changes of $\Delta x_{min} = 5$ μm given by the resolution of the micrometer screw (from the linear dependencies derived from Fig. 5 and mentioned in Sec. II B, this applies for blue-shifts and red-shifts in stretching and relaxation directions, respectively). But there is nothing to be said against improving this by using finer mechanical-tuning devices. Also we want to emphasize that the shown approach of resonance tuning is entirely reversible. This is illustrated in Fig. 4(b) in more detail where we stacked the PL spectra recorded before the stretching process and after relaxation of the substrate. Clearly, the modes are located at the same spectral positions with a measured average deviation of 5.9 pm that is within the uncertainty of the mode determination from Lorentzian fits (6.6 pm).
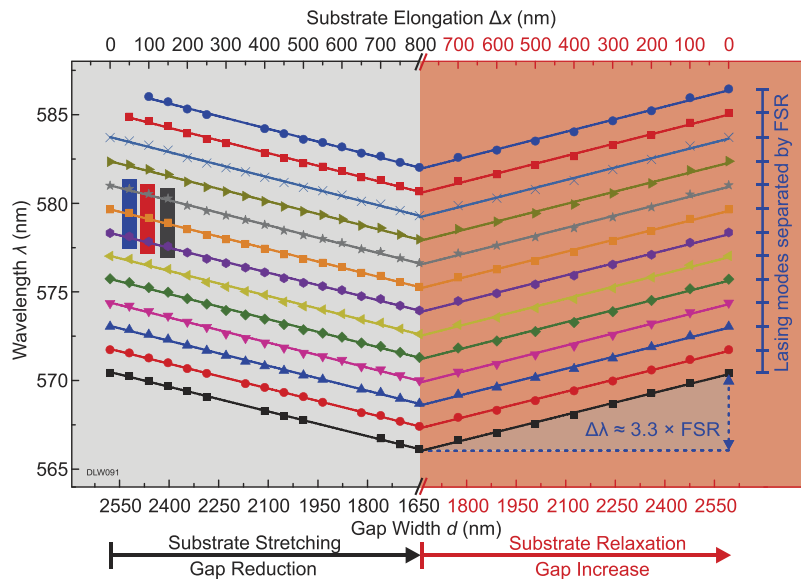

FIG. 5. Demonstration of reversible resonance tuning for split-disks on elastomer substrates: The spectral positions of lasing modes separated by the free spectral range are plotted in dependence of the derived coupling gap size d in differently colored symbols. A second x-axis on the top shows the dependence on the substrate elongation Δx. The left part (shaded in grey) corresponds to a gap reduction (substrate stretching) inducing a blue-shift of all resonances. Subsequent relaxation of the substrate strain results in a gap increase and complete reversal of the spectral shifts (right part, shaded in red). A total gap change of $\Delta d = 920$ nm corresponding to wavelength tuning of $\Delta\lambda_{tot} = 4.4$ nm $\hat{=}$ $3.3 \times$ FSR is identified. As expected, the modal shift is linearly dependent on the gap size and the substrate elongation. Straight lines have been fitted to the data. The lasing modes corresponding to the spectra shown in Fig. 4(a) are shaded in corresponding colors.

The large reversible tuning of laser modes and its linear dependence on the gap size throughout the whole substrate elongation are demonstrated by evaluation of the collected data presented in Fig. 5. Here we focus on the laser modes that can be tracked over the whole tuning range. Similarly as for the micro-lasers with fixed gaps, a shift of the lasing envelope occurs upon variation of the gap and additional lasing modes can be observed at higher wavelengths for reduced gap widths and smaller wavelengths for enlarged gap widths, respectively. For clarity of the graph, we do not include them in Fig. 5. They show the same wavelength trends as the presented modes.

The spectral positions of the laser modes (as deduced from the line-shape fits) are represented by differently colored symbols. In the left part of the figure (shaded in grey), one can follow the simultaneous linear blue-shift of all lasing peaks as a function of the decreasing gap width. Relaxing the strain of the substrate and thus opening again the gap between the two halves of the resonator leads to a complete reversal of the modal shifts. Over the tuning range of the gap reported here, we find a total shift of the lasing modes of a multiple of the free spectral range ($\Delta\lambda_{\text{tot}}$ = 4.4 nm $\hat{=}$ 3.3 × FSR). The presented data demonstrate the functionality of split-disks on elastomer substrates as widely tunable photonic devices.

The presented split-disk geometry might be also useful for applications other than resonance tuning, e.g., for tunable coupled resonator optical waveguides or for enhanced sensing performance in sensing applications. First proof-of principle experiments towards the application of the split-disk geometry for enhanced sensing look very promising and are attached in the supplementary material.

IV. CONCLUSIONS

In summary, we have realized a novel type of a WGM micro-resonator which allows a large reversible resonance tuning. The cavities consist of opposing polymeric half-disks with an intermediate coupling gap. Detailed investigation of the figures of merit of such devices has been performed on polymeric dye-doped split-disks fabricated with electron beam lithography on silicon substrates. The changes in lasing threshold and quality factor upon enlarging the gap width reflect the related increase of cavity losses while low-threshold lasing is still maintained. For resonator tunability we exploit the flexible deformation of the elastomer PDMS which is used as substrate for split-disks fabricated by direct laser writing. Fine-tuning of the cavity modes is evoked by tuning of the split-disk gap upon lateral contraction when the substrate is stretched. Linear tunability of the lasing modes over more than three times the free spectral range has been observed including full reversibility.

To evaluate the tuning performance of split-disk resonators, we shortly compare our approach with the described tuning methods for elastomeric DFB lasers (see Introduction). On the one hand, the total tuning range evoked by split-disks is smaller compared to the tuning ranges reported for elastomeric DFB lasers (Li *et al.* reported a tuning range of nearly 60 nm,[34] Döring *et al.* showed a 50 nm tuning range[37]). On the other hand, however, the presented method is superior regarding fine-tuning. The mentioned differences originate from the fact that for DFB lasers the grating pitch is varied along the substrate deformation direction, whereas for tuning in split-disk cavities the smaller lateral substrate deformation is exploited.

The reported tunable cavities open the path towards highly flexible and variable photonic architectures. In particular, tuning of light-matter coupling by matching resonances of cavities with quantum-emitter transitions or switching of super-mode propagation in photonic molecules or cavity arrays are feasible.

SUPPLEMENTARY MATERIAL

See supplementary material for supporting content.

ACKNOWLEDGMENTS

[1] K. J. Vahala, Nature **424**, 839 (2003).
[2] D. G. Lidzey, D. D. C. Bradley, M. S. Skolnick, T. Virgili, S. Walker, and D. M. Whittaker, Nature **395**, 53 (1998).
[3] M. J. Hartmann, F. G. S. L. Brandão, and M. B. Plenio, Laser Photonics Rev. **2**, 527 (2008).
[4] T. J. Kippenberg, H. Rokhsari, T. Carmon, A. Scherer, and K. J. Vahala, Phys. Rev. Lett. **95**, 033901 (2005).
[5] Y.-S. Park and H. Wang, Opt. Express **15**, 16471 (2007).
[6] A. M. Armani, R. P. Kulkarni, S. E. Fraser, R. C. Flagan, and K. J. Vahala, Science **317**, 783 (2007).
[7] D. V. Guzatov and U. Woggon, Appl. Phys. Lett. **94**, 241104 (2009).
[8] M. A. Santiago-Cordoba, S. V. Boriskina, F. Vollmer, and M. C. Demirel, Appl. Phys. Lett. **99**, 073701 (2011).
[9] V. Duong Ta, R. Chen, L. Ma, Y. Jun Ying, and H. Dong Sun, Laser Photonics Rev. **7**, 133 (2013).
[10] M. R. Foreman, J. D. Swaim, and F. Vollmer, Adv. Opt. Photonics **7**, 168 (2015).
[11] A. Polman, B. Min, J. Kalkman, T. J. Kippenberg, and K. J. Vahala, Appl. Phys. Lett. **84**, 1037 (2004).
[12] T. Grossmann, S. Schleede, M. Hauser, M. B. Christiansen, C. Vannahme, C. Eschenbaum, S. Klinkhammer, T. Beck, J. Fuchs, G. U. Nienhaus, U. Lemmer, A. Kristensen, T. Mappes, and H. Kalt, Appl. Phys. Lett. **97**, 063304 (2010).
[13] R. Chen, B. Ling, X. W. Sun, and H. D. Sun, Adv. Mater. **23**, 2199 (2011).
[14] S. Xiao, M. H. Khan, H. Shen, and M. Qi, Opt. Express **15**, 14765 (2007).
[15] Q. Xu, B. Schmidt, S. Pradhan, and M. Lipson, Nature **435**, 325 (2005).
[16] P. Rabiei, S. Member, W. H. Steier, L. Fellow, C. Zhang, and L. R. Dalton, J. Lightwave Technol. **20**, 1968 (2002).
[17] S. Yang, Y. Wang, and H. Sun, Adv. Opt. Mater. **3**, 1136 (2015).
[18] J. P. Reithmaier, G. Sęk, A. Löffler, C. Hofmann, S. Kuhn, S. Reitzenstein, L. V. Keldysh, V. D. Kulakovskii, T. L. Reinecke, and A. Forchel, Nature **432**, 197 (2004).
[19] K. Hennessy, A. Badolato, M. Winger, D. Gerace, M. Atatüre, S. Gulde, S. Fält, E. L. Hu, and A. Imamoğlu, Nature **445**, 896 (2007).
[20] K. Vahala, *Optical Microcavities* (World Scientific, Singapore, 2004).
[21] B. Peng, Ş. K. Özdemir, J. Zhu, and L. Yang, Opt. Lett. **37**, 3435 (2012).
[22] R. M. Waxler, D. Horowitz, and A. Feldman, Appl. Opt. **18**, 101 (1979).
[23] K. Djordjev, S. Choi, S. Choi, and P. D. Dapkus, IEEE Photonics Technol. Lett. **14**, 828 (2002).
[24] W. Zhang and J. Yao, APL Photonics **1**, 080801 (2016).
[25] I. Chremmos, O. Schwelb, and N. Uzunoglu, *Photonic Microresonator Research and Applications* (Springer, New York, 2010).
[26] S. Irmer, J. Daleiden, V. Rangelov, C. Prott, F. Römer, M. Strassner, A. Tarraf, and H. Hillmer, IEEE Photonics Technol. Lett. **15**, 434 (2003).
[27] E. C. Vail, G. S. Li, W. Yuen, and C. J. Chang-Hasnain, IEEE J. Sel. Top. Quantum Electron. **3**, 691 (1997).
[28] F. Chollet, Micromachines **7**, 18 (2016).
[29] M.-C. M. Lee and M. C. Wu, Opt. Lett. **31**, 2444 (2006).
[30] M.-C. M. Lee and M. C. Wu, Opt. Express **14**, 4703 (2006).
[31] E. Gil-Santos, C. Baker, A. Lemaître, C. Gomez, G. Leo, and I. Favero, Nat. Commun. **8**, 14267 (2017).
[32] V. D. Ta, R. Chen, and H. D. Sun, Sci. Rep. **3**, 1362 (2013).
[33] A. M. Flatae, M. Burresi, H. Zeng, S. Nocentini, S. Wiegele, C. Parmeggiani, H. Kalt, and D. Wiersma, Light: Sci. Appl. **4**, e282 (2015).
[34] Z. Y. Li, Z. Y. Zhang, T. Emery, A. Scherer, and D. Psaltis, Opt. Express **14**, 696 (2006).
[35] B. Wenger, N. Tétreault, M. E. Welland, and R. H. Friend, Appl. Phys. Lett. **97**, 193303 (2010).
[36] P. Görrn, M. Lehnhardt, W. Kowalsky, T. Riedl, and S. Wagner, Adv. Mater. **23**, 869 (2011).
[37] S. Döring, M. Kollosche, T. Rabe, J. Stumpe, and G. Kofod, Adv. Mater. **23**, 4265 (2011).
[38] T. Beck, S. Schloer, T. Grossmann, T. Mappes, and H. Kalt, Opt. Express **20**, 22012 (2012).
[39] T. Siegle, S. Schierle, S. Kraemmer, B. Richter, S. F. Wondimu, P. Schuch, C. Koos, and H. Kalt, Light: Sci. Appl. **6**, e16224 (2017).
[40] T. M. Siegle, M. Remmel, S. Krämmer, and H. Kalt, in *Conference on Lasers Electro-Optics, OSA Technical Digest (online)* (Optical Society of America, San Jose, USA, 2017), paper SM2N.4.
[41] T. Grossmann, M. Hauser, T. Beck, C. Gohn-Kreuz, M. Karl, H. Kalt, C. Vannahme, and T. Mappes, Appl. Phys. Lett. **96**, 013303 (2010).
[42] H. Chandrahalim and X. Fan, Sci. Rep. **5**, 18310 (2015).
[43] G. C. Righini, Y. Dumeige, P. Feron, M. Ferrari, G. N. Conti, D. Ristic, and S. Soria, Riv. Nuovo Cim. **34**, 435 (2011).
[44] T. Grossmann, T. Wienhold, U. Bog, T. Beck, C. Friedmann, H. Kalt, and T. Mappes, Light: Sci. Appl. **2**, e82 (2013).
[45] M. Mazumder, G. Chen, and R. K. Chang, Opt. Lett. **20**, 878 (1995).
[46] S. K. Y. Tang, R. Derda, Q. Quan, M. Lončar, and G. M. Whitesides, Opt. Express **19**, 2204 (2011).
[47] S. Krämmer, S. Rastjoo, T. Siegle, S. F. Wondimu, C. Klusmann, C. Koos, and H. Kalt, Opt. Express **25**, 7884 (2017).
[48] T. Grossmann, S. Schleede, M. Hauser, T. Beck, M. Thiel, G. von Freymann, T. Mappes, and H. Kalt, Opt. Express **19**, 11451 (2011).
[49] M. A. Albota, C. Xu, and W. W. Webb, Appl. Opt. **37**, 7352 (1998).
[50] G.-M. Parsanasab, M. Moshkani, and A. Gharavi, Opt. Express **23**, 8310 (2015).